DEUTSCHES ELEKTRONEN-SYNCHROTRON DESY

DESY SR-75/06
May 1975

Ultraviolet Photoemission Spectroscopy of Solid Nitrogen and Oxygen

by

F.-J. Himpsel and N. Schwentner
Sektion Physik der Universität München

E. E. Koch
Deutsches Elektronen-Synchrotron DESY, Hamburg

2 HAMBURG 52 · NOTKESTIEG 1

To be sure that your preprints are promptly included in the
HIGH ENERGY PHYSICS INDEX ,
send them to the following address (if possible by air mail) :

DESY
Bibliothek
2 Hamburg 52
Notkestieg 1
Germany

Ultraviolet Photoemission Spectroscopy of Solid Nitrogen and Oxygen*

F.-J. Himpsel and N. Schwentner

Sektion Physik der Universität München, 8 München 40, Germany

and

E. E. Koch

Deutsches Elektronen-Synchrotron DESY, 2 Hamburg 52, Germany

* Research supported in part by the Deutsche Forschungsgemeinschaft DFG and by the Bundesministerium für Forschung und Technologie BMfT.

ABSTRACT:

Photoelectron energy distribution curves and constant final state spectra of polycrystalline films of solid N_2 and O_2 have been measured for photon energies 10 eV $\leq \hbar\omega \leq$ 30 eV by use of synchrotron radiation. Varying the photon energy and final state energy respectively the observed transitions originating from the valence bands could be attributed to the known molecular orbitals (MO's) of the gaseous samples. The binding energies of the various MO's are lowered by 1.5 eV for solid N_2 and 1.6 eV for solid O_2. This is explained by electronic relaxation via the dielectric polarization of the medium. Results on other nonpolar molecular crystals are included to check a simple estimate of the polarization energy based on the Mott-Littleton model.

ZUSAMMENFASSUNG:

Energieverteilungskurven der Photoelektronen und Photoemissionsspektren mit fester Endenergie wurden für polykristalline N_2 und O_2 Schichten für Photonenenergien 10 eV $\leq \hbar\omega \leq$ 30 eV mit Synchrostronstrahlung gemessen.Durch die Variation der Photonenenergie bzw. der Energie des festen Endzustands konnten die beobachteten Übergänge aus den Valenzbändern bekannten Molekülorbitalen der gasförmigen Substanzen zugeordnet werden. Die Bindungsenergien der verschiedenen Molekülorbitale sind um 1.5 eV für festes N_2 und um 1.6 eV für festes O_2 niedriger. Diese Verschiebungen lassen sich auf Grund der elektronischen Relaxation durch die dielektrische Polarisation des Mediums erklären. Es werden Ergebnisse für andere nicht polare Mülekülkristalle herangezogen, um eine einfache Abschätzung der Polarisationsenergie auf Grund des Mott-Littleton-Modells zu prüfen.

1. INTRODUCTION

In molecular crystals the covalent binding within the molecules exceeds by far the van der Waals and multipole forces responsible for the crystalline order. Thus one expects in the condensed phase excited electronic states similar to those of the free molecule. In fact for solid atmospheric gases it was possible to attribute bound states below the band gap, observed by optical absorption[1], reflection [2] and electron energy loss spectroscopy[3] to electronic excitations of the free molecule using exciton models. In addition deperturbation effects on the valence shell excitations have been observed for the solid phase due to the strong quenching of energetically degenerate Rydberg states by the solid environment[1b]. In the range of continuum excitations however, optical spectroscopy generally yields a rather indirect information averaging over different transitions, whereas photoelectron spectroscopy allows to separate initial and final state contributions.

In the present paper we report on extensive photoemission experiments for solid N_2 and O_2 and on some results for solid CO_2 and CH_4. The detailed new information obtained may be useful for a better interpretation of the optical spectra, for establishing the electronic band structure of these solids and finally, in connection with results of recent charge transport measurements[4] may lead to an improved understanding of secondary effects, such as the electron phonon interaction in these molecular crystals.

2. EXPERIMENT

Research grade gases (L'Air Liquide, 99, 9992 % purity) were condensed under UHV conditions (pressure before and after condensation $1 \cdot 10^{-10}$ Torr) on a helium cooled gold substrate. The temperature of the substrate, being in the 40 to 50 K range, presumable favoured the growth of polycrystalline films of the high temperature phases. The film thickness d was measured by an in situ interferometric method. It was kept below 200 Å in order to avoid potential shifts due to sample charging, and varied between 30 and 300 Å in oder to ascertain that the observed photoemission represents the bulk properties of the condensed films. A smooth struc tureless contribution to the photo-

emission of hot electrons originating from the gold substrate was only observed for films with thicknesses below 50 Å.

As a broad-band Vaccum Ultraviolet light source we used the DESY-electron accelerator. The photoelectron energy analyzer, a combination of electrostatic lenses and a retarding grid, was mounted normal to the sample surface with an angle of acceptance of 3°. The energy calibration was performed by the zero kinetic energy onset of the spectra with an error of 0.2 eV. This number also allows for small uncertainties due to charging. The spectra were recorded digitally. For further details of the experiment see reference [5].

3. RESULTS

For solid N_2 the photoelectron energy distribution curves (EDC's) show three initial state structures, labelled A, B, C in Fig. 1, originating from the valence bands and secondary electrons concentrated in a final state near the vacuum level (peak D). For an exciting photon energy near 21 eV comparison is made between photoelectron spectra for gaseous [6a] and condensed N_2 (in Fig. 2). The energy scales have been shifted in such a way that the adiabatic ionization potential (IP_{ad}) of the uppermost ($3\sigma_g$) molecular orbital coincides with the onset of the first EDC band (A) from the solid. This rigid shift of the energy scale leads to an alignment of the adiabatic IP's for the other bands too, yielding a value of 1.5 eV for this shift.(see also Fig. 5). This will be discussed below.

For solid O_2 the valence band structures in the EDC's interfere with a maximum in the density of final states approximately 2 eV above the vacuum level (Fig. 3). In order to separate these final state effects from the EDC's we have measured constant final state spectra by continuous variation of the exciting photon energy. The results for various final state energies are displayed in Fig. 4. The onsets of the photoemission out of different valence bands are marked by the dashed lines and compared with the molecular adiabatic ionization limits [6a,6b]. Neglecting final state dependent structures we are able to establish again a one to one correspondence between EDC bands from the solid and the states of the free ion. This

implies a reduction of the ionization energies by a value of 1.6 eV similar to the one obtained for N_2 (see also Fig. 5).

In similar but preliminary experiments for solid CO_2 we observed a gas to solid shift of -1.5 eV for the first and second IP and for solid CH_4 a value of about -1.2 eV. In CH_4 final state structure is visible up to 4 eV above the vacuum level.

4. DISCUSSION

4.1 Valence bands and hole polarization

The assignment of the EDC bands to the various molecular orbitals as described in Section 3 and compiled in Fig. 5 gives an overall picture of the energies involved for the valence bands of solid N_2 and O_2 except for the lowest bands not covered by the present experiments. In absence of band structure calculations for these molecular crystals we discuss in the following the gas to solid shifts of the binding energies within the framework of the Mott-Littleton model.

The electronic relaxation in a solid has been discussed in detail by several authors[7] in order to explain reduced ionization potentials in the solid. Applying this concept to van der Waals insulators we suggest that the dielectric polarization around the hole is the main relaxation mechanism. To account for this contribution we have estimated the hole polarization energy P_+ in a simple continuum model. We assume that the electronic part of the polarization follows adiabatically the escape of the photoelectron. Suppose the interior of the hole represented by a sphere in a close packed structure has the same charge distribution as the free ion. Then we get for P_+ as the energy difference between the screened hole and the free ion:

$$P_+ = \left(\frac{1}{2}\int \mathrm{ED}\ \mathrm{dV}\right)\Big/_{\text{Solid}}^{\text{Gas}} = \frac{e^2}{8\pi\varepsilon_o}\left(1 - \frac{1}{\varepsilon_{el}}\right)\cdot\frac{1}{r} \qquad (1)$$

where ε_{el} is the electronic dielectric constant and 2r the nearest neighbour distance.

In Table I and Fig. 6 we compare calculated values for P_+ with available ex-

perimental gas to solid shifts of the adiabatic ionization potentials. ε_{el} was calculated using the refractive index n in the visible (full circles in Fig. 6) i.e. for frequencies which correspond to the escape time of the photoelectron. In absence of such data we used the Clausius-Mosotti formula. For anisotropic crystals the nearest neighbour distance 2r has been averaged over the 12 nearest neighbours. It is evident that the magnitude of the shift is given correctly by this procedure. Thus one may estimate the valence band positions of a wide class of molecular crystals. The limitations of the above model become obvious for condensed phases of polar molecules. Recent preliminary experiments for H_2O and NH_3 [13] resulted in higher polarization energies probably due to additional short range relaxation in the solid. Furthermore the observation of different gas to solid shifts for different orbitals indicates such a process.

4.2 Conduction bands

The final state density maximum in O_2, manifested by the enhancement of the EDC curves at 2 to 3 eV final state energy (see Fig. 3), has been confirmed by yield measurements. From threshold at 10.8 eV the yield remains in the order of 10^{-3} electrons per photon up to a second quadratic threshold at 12.5 eV, where it rises by more than one order of magnitude. This indicates two conduction bands starting at 0.3 eV and 2.0 eV above the vacuum level. Using the obtained band structure features one may get more insight into the optical data.

4.3 Electron-phonon interaction

The rather sharp peak of secondaries near the vacuum level observed for solid N_2 and O_2 may be explained in a way proposed by Chang and Berry [4b]. As long as an electron has enough energy to excite an internal vibration of the molecule corresponding to an optical phonon, it undergoes strong inelastic scattering. Below this threshold the mean free path increases. This can be seen e.g. in the EDC's of solid N_2: the peak of the scattered electrons grows with increasing sample thickness up to several hundred Å whereas the intensity of the more energetic photoelectrons reaches saturation well below 100 Å.

Another phonon process can be inferred from Fig. 2. The occurance of rather broad bands in the EDC of the solid is explained to a substantial part by the excitation of internal vibrations at the created hole [14]. This leads to a line shape similar to the envelope of the EDC from the gas although the individual vibrational lines could not be resolved. We note, that in addition to the limited experimental resolution, bending of the valence bands within the Brillouin zone will also contribute to a broadening of the fine structure in the observed EDC's.

5. ACKNOWLEDGEMENTS

We thank W. Steinmann for his interest and support of this work and J. Jortner and V. Saile for stimulating discussions.

TABLE 1: Comparison of experimental gas to solid shifts ($P_{+\ exp}$) with calculated values ($P_{+\ th}$) according to eq. (1) for a number of molecular crystals. Values in brackets have been calculated using the Clausius Mosotti formula.

Substance	$P_{+\ exp}$ [eV]	Ref	$\langle\varepsilon\rangle_{el}$	Ref	$\langle r\rangle$ [Å]	Ref	$P_{+\ th}^{*}$ [eV]
Ne	1.3	8	1.51	12a	1.58	10d	1.54
Ar	1.8	8	1.69	12b	1.88	10d	1.57
Kr	2.0	8	1.90	12b	2.00	10d	1.71
Xe	2.2	8	2.25	12b	2.17	10d	1.83
N_2	1.5	*	1.49	12a	2.0	11	1.2
O_2	1.6	*	1.56	12a	1.7	10a,11	1.5
CO_2	1.5	*	1.49	12a	2.0	11	1.2
CH_4	1.2	*	(1.80)	11	2.08	11	(1.54)
C_2H_4	1.7	9	(2.25)	11	1.82	11	(2.20)
C_2H_2	1.5	9	(1.92)	11	2.17	11	(1.59)
C_6H_6	1.4	9	2.5	12c	2.8	11,12c	1.5

* : this work

Referecnes

1a M. Brith, O. Schnepp, Mol. Phys. 9, 473 (1965)

1b E. Boursay and J.Y. Roncin, Phys. Rev. Letters 26,308 (1971)

2a R.A.H. Buxton and W.W. Duley, Phys. Rev. Letters 25,801 (1970)

2b R. Haensel, E.E. Koch, N. Kosuch, U. Nielsen, and M. Skibowski, Chem. Phys. Letters 9,548 (1971)

2c S.R. Scharber, S.E. Webber, J. Chem. Phys. 55,3977 (1971)

3a J. Daniels, Opt. Comm. 2,352 (1970)

3b H.J. Hinz, in: Vacuum Ultraviolet Radiation Physics, edited by E.E. Koch, R. Haensel and C. Kunz, Vieweg-Pergamon (1974), p.176

4a R.J. Loveland, P.G. Le Comber, and W.E. Spear, Phys. Rev. B6,3121 (1972) and B11,3124 (1975)

4b Y.C. Chang, W.B. Berry, J. Chem. Phys. 61,2727 (1974)

5 N. Schwentner, E.E. Koch, V. Saile, M. Skibowski, A. Harmsen, in: Vacuum Ultraviolet Radiation Physics, edited by E.E. Koch, R. Haensel and C. Kunz, Vieweg-Pergamon (1974), p.792

6a D.W. Turner, C. Baker, A.D. Baker, and C.R. Brundle, Molecular Photoelectron Spectroscopy, Wiley, New York (1970)

6b W.C. Price, A.W. Polts and D.G. Streets, in Electron Spectroscopy, eidted by D.A. Shirley,North Holland, Amsterdam (1972), p.187

7a N.F. Mott, M.J. Littleton, Trans. Faraday Soc. 34,485 (1938)

7b W.B. Fowler, Phys. Rev. 151,657 (1966)

7c D.A. Shirley, Chem. Phys. Lett. 16,220 (1972)

7d P.H. Citrin, O.R. Hamann, Chem. Phys. Lett. 22,301 (1973)

8 N. Schwentner, F.-J. Himpsel, V. Saile, M. Skibowski, W. Steinmann, and E.E. Koch, Phys. Rev. Letters 34,528 (1975)

9 J.E. Demuth and D.E. Eastman, Phys. Rev. Letters 32,1123 (1974)

10a C.S. Barrett, L. Meyer, and J. Wasserman, J. Chem. Phys. 47,592 (1967)

10b C.A. English and J.A. Venables, Proc. Roy. Soc. Lond. A340,57 (1974)

10c C.A. English and J.A. Venables, Proc. Roy. Soc. Lond. A340,81 (1974)

10d G.L. Pollack, Rev. Mod. Phys. 36,748 (1964)

11 Landolt-Börnstein, I/3, Springer (1951); and II/5a, Springer (1971); and III/6, Springer (1971),
and Amercian Institute of Physics Handbook, McGraw-Hill (1957)

12a J. Kruger, W.J. Ambs, J. Opt. Soc. Am. 49,1195 (1959)

12b A.C. Sinnock, B.L. Smith, Phys. Rev. 181,1297 (1969)

12c V.L. Broude, Sov. Phys. Usp. 4,584 (1962)

13 F.-J. Himpsel, unpublished data

14 see e.g. the discussion by P.H. Citrin, P. Eisenberger, and D.R. Hamann, Phys. Rev. Letters 33,965 (1974)

Figure Captions:

Fig. 1: Photoelectron energy distributions of solid N_2 versus initial energy for various energies of the exciting photon. The diagonal line marks zero kinetic energy. Features originating from the same initial state are aligned vertically.

Fig. 2: Comparison of photoelectron spectra for gaseous [6a] and condensed N_2 for $\hbar\omega \approx 21$ eV. The energy scales have been shifted to let the adiabatic ionization energies (dashed lines) coincide.

Fig. 3: Photoelectron energy distributions of solid O_2 versus initial energy for various energies of the exciting photon (same plot as in Fig. 1). The dashed diagonal lines mark final energies 0 eV, 2 eV and 4 eV respectively.

Fig. 4: Constant final state spectra of solid O_2, compared with the photoelectron spectrum of the gaseous phase [6]. The zero line for each curve is shifted proportional to the kinetic energy of the electron kept fixed for each scan, while the photon energy $\hbar\omega$ was varied. Onsets of photoemission out of different valence bands are marked by dashed lines and compared with the adiabatic JP's of the molecule.

Fig. 5: Adiabatic JP's for gaseous [6] and solid (this work) N_2 and O_2. The one electron MO assignments are given.

Fig. 6: Comparison of calculated hole polarization energies with experimental solid to gas shifts of the adiabatic JP's. For details see text. The references are the same as for Table 1.

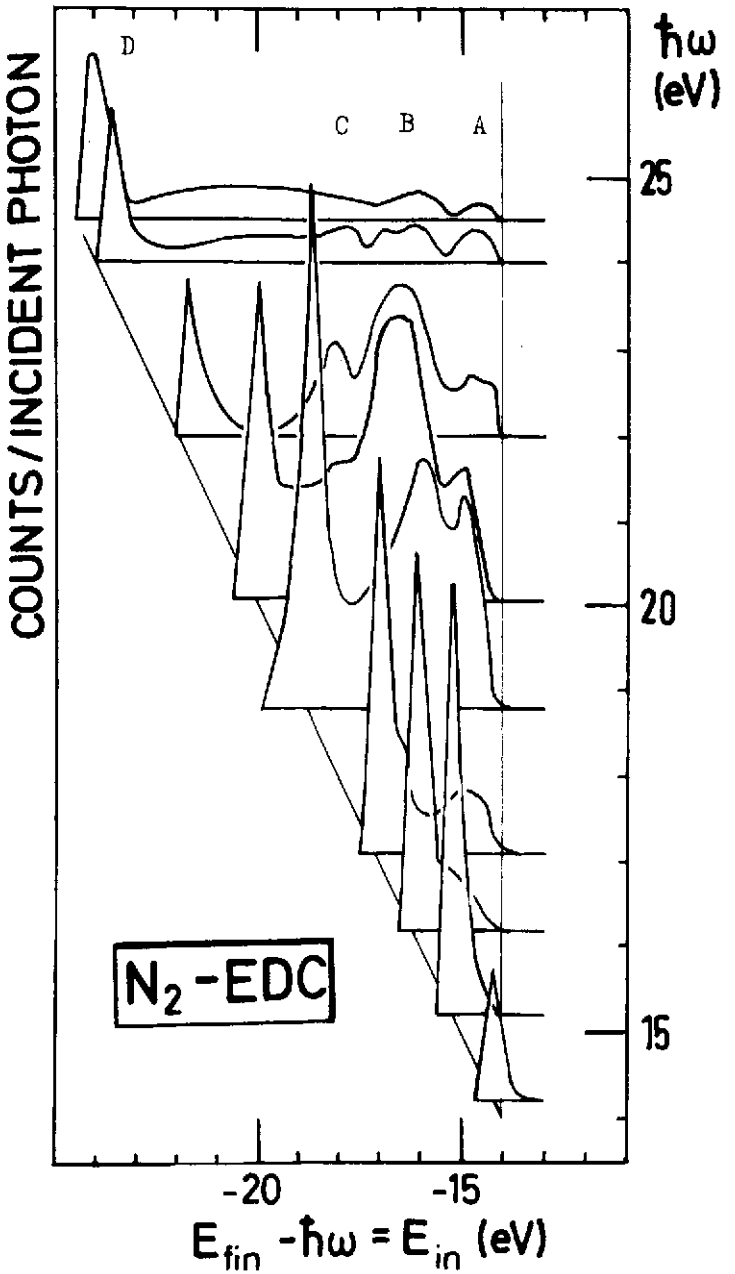
COUNTS/INCIDENT PHOTON
D
C
B
A
ħω (eV)
25
20
15
N2 - EDC
-20
-15
Efin - ħω = Ein (eV)

Fig.1

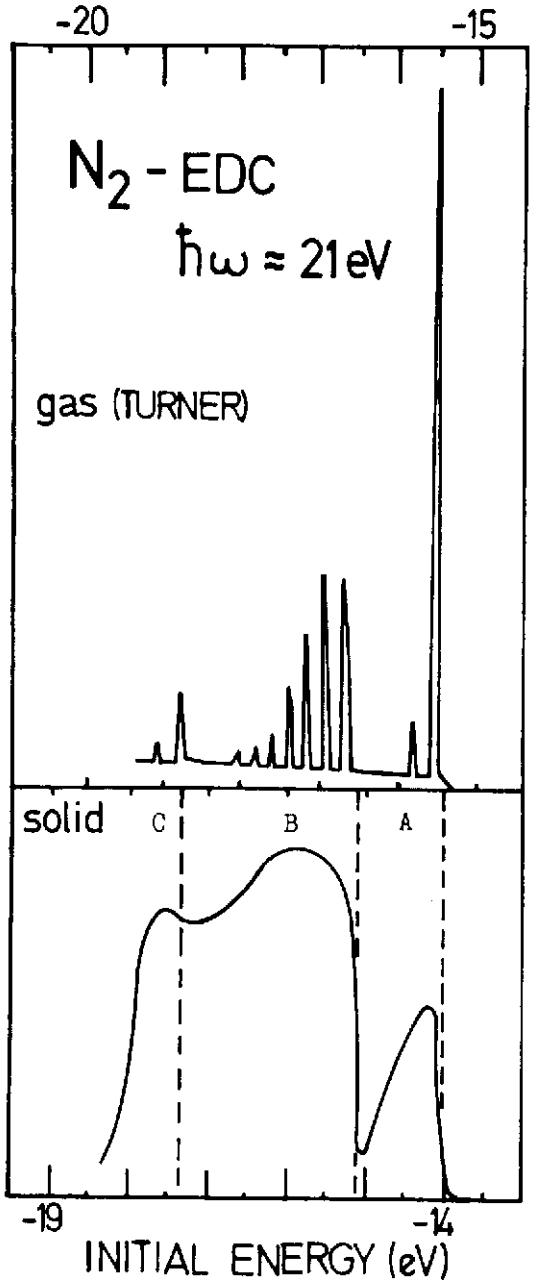
-20
-15
N2 - EDC
ħω ≈ 21 eV
gas (TURNER)
solid
C
B
A
-19
-14
INITIAL ENERGY (eV)

Fig.2

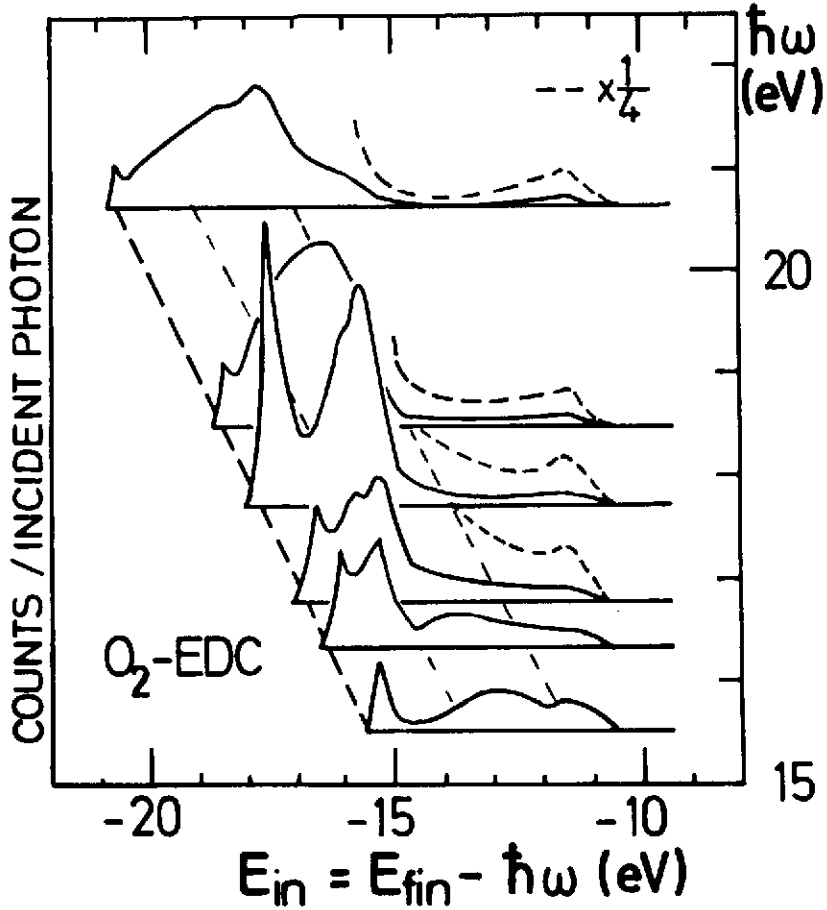
ħω (eV)
-- x1/4
20
15
COUNTS / INCIDENT PHOTON
O2-EDC
-20
-15
-10
Ein = Efin - ħω (eV)

Fig.3

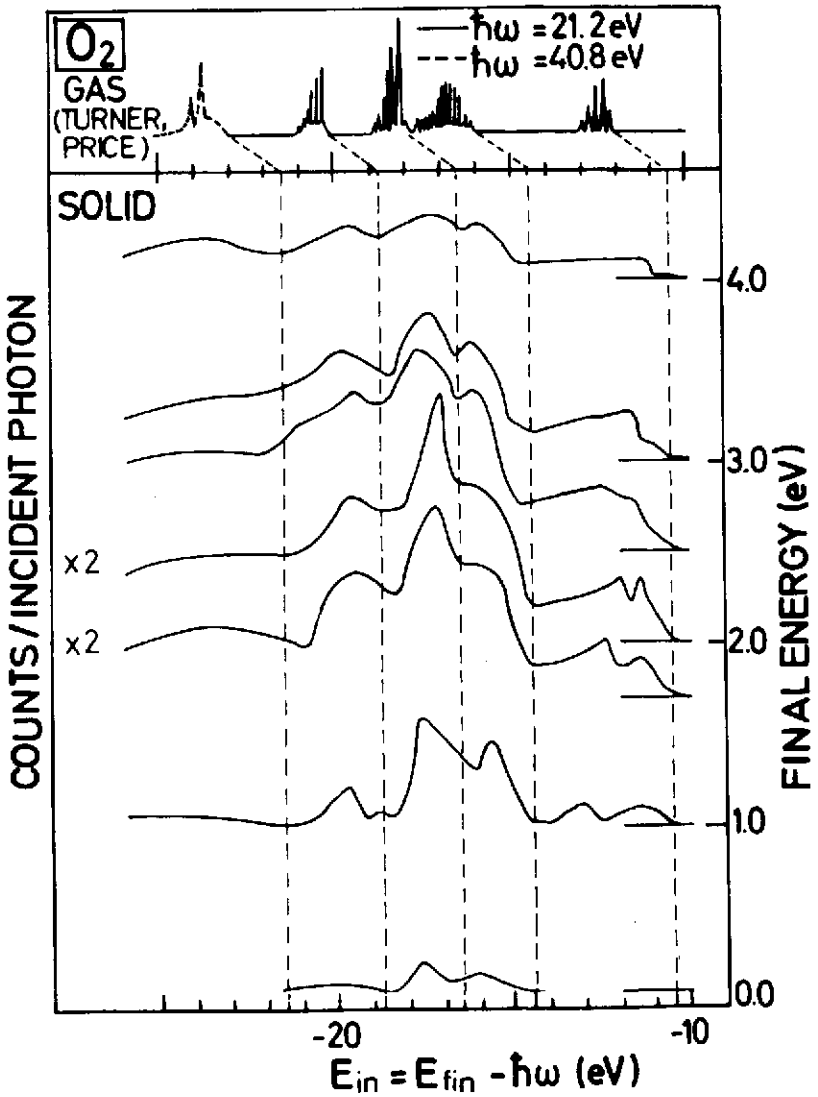
O2
GAS
(TURNER, PRICE)
ħω =21.2eV
ħω =40.8eV
SOLID
4.0
3.0
x2
x2
2.0
1.0
0.0
COUNTS/INCIDENT PHOTON
FINAL ENERGY (eV)
-20
-10
Ein = Efin - ħω (eV)

Fig.4

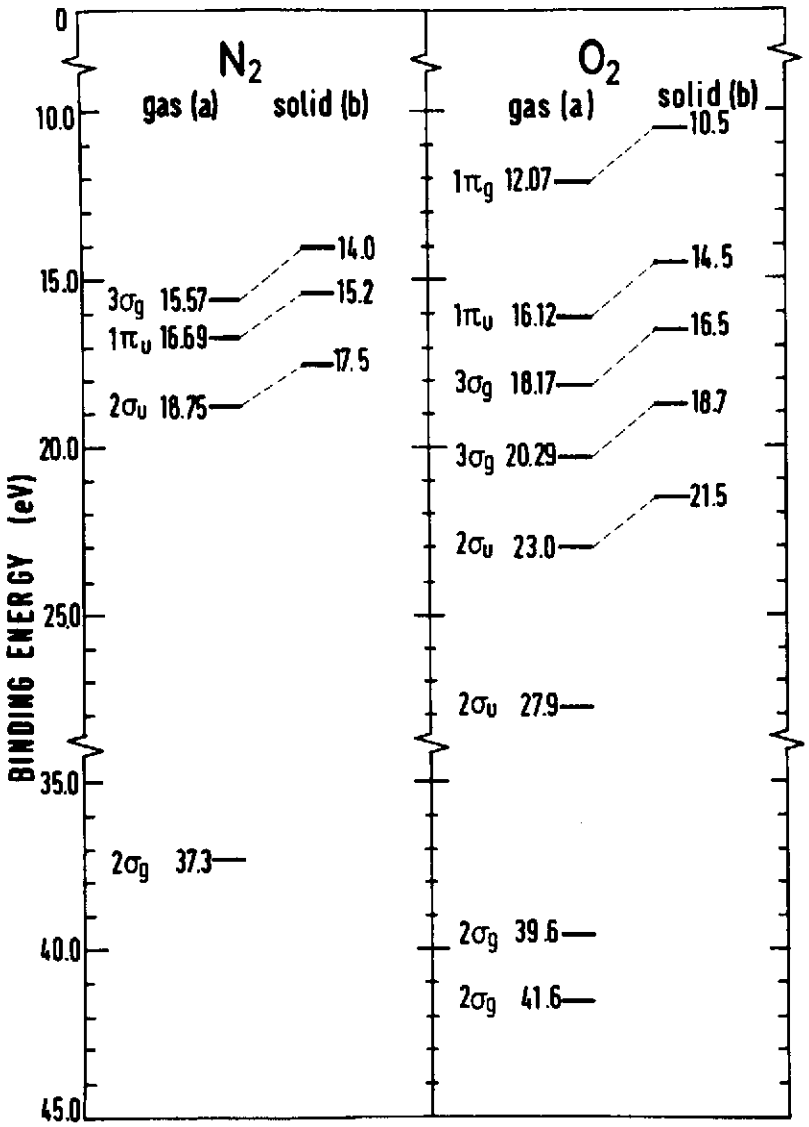
N2
gas (a)
solid (b)
O2
gas (a)
solid (b)
BINDING ENERGY (eV)
0
10.0
15.0
20.0
25.0
35.0
40.0
45.0
3σg 15.57
1πu 16.69
2σu 18.75
2σg 37.3
14.0
15.2
17.5
1πg 12.07
1πu 16.12
3σg 18.17
3σg 20.29
2σu 23.0
2σu 27.9
2σg 39.6
2σg 41.6
10.5
14.5
16.5
18.7
21.5

Fig.5

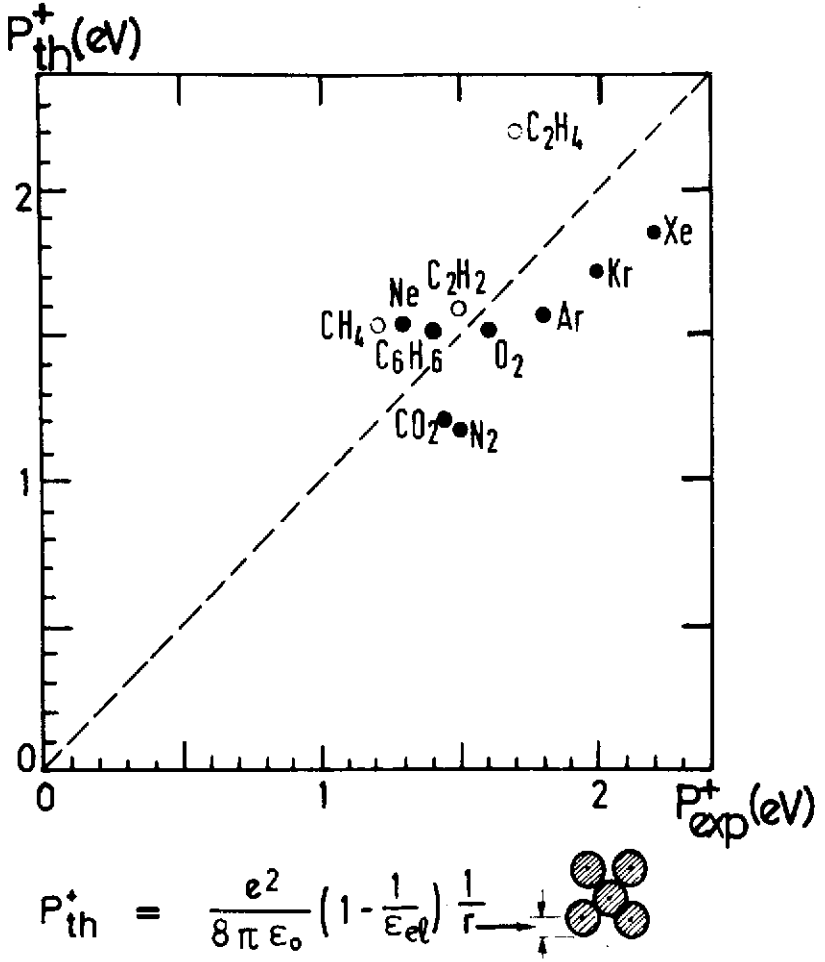
P+th(eV)
P+exp(eV)
0
1
2
C2H4
Xe
Kr
Ne
C2H2
CH4
Ar
C6H6
O2
CO2
N2
P+th = e2/8πε0 (1 - 1/εel) 1/r

Fig.6